American Mineralogist, Volume 68, pages 41–59, 1983

Phase transitions and decomposition relations in calcic plagioclase

TIMOTHY L. GROVE

Department of Earth and Planetary Sciences
Massachusetts Institute of Technology
Cambridge, Massachusetts 02139

JOHN M. FERRY

Department of Geology
Arizona State University
Tempe, Arizona 85287

AND FRANK S. SPEAR

Department of Earth and Planetary Sciences
Massachusetts Institute of Technology
Cambridge, Massachusetts 02139

Abstract

A subsolidus temperature–composition diagram for the calcic portion of the system $NaAlSi_3O_8$–$CaAl_2Si_2O_8$ is derived from the following data: (a) compositions of plagioclase crystallized under a range of metamorphic conditions; (b) TEM observations of coexisting andesine (An_{39}) and bytownite (An_{88}); and (c) TEM and crystallographic studies of calcic plagioclase from the literature. The most significant feature of the diagram is a proposed existence of two tricritical points and their associated conditional spinodals. One tricritical point is a consequence of the $C\bar{1} \rightleftarrows I\bar{1}$ transition, which is inferred, from microstructures of plutonic plagioclase, to occur near An_{73}–An_{75} at ~900°C. The other tricritical point is a consequence of the $I\bar{1} \rightleftarrows P\bar{1}$ transition and is inferred to be located near An_{75}–An_{78} at ~675°C. The $C\bar{1} \rightleftarrows I\bar{1}$ conditional spinodal is responsible for submicroscopic two-phase intergrowths in labradorites and for Bøggild intergrowths (An_{45}–An_{65}). The $I\bar{1} \rightleftarrows P\bar{1}$ conditional spinodal is responsible for Huttenlocher intergrowths (An_{66}–An_{87}). At temperatures between ~400° and ~575°C, plagioclase in the range of bulk composition An_{40}–An_{90} should produce an equilibrium oligoclase/andesine + bytownite assemblage by nucleation and growth. Intermediate compositions are interpreted to be the result of metastable plagioclase growth and/or decomposition to submicroscopic intergrowths within either of the two conditional spinodals. Even the long equilibration times associated with regional metamorphism fail to produce equilibrium plagioclase feldspar compositions.

Introduction

The topology of the subsolidus temperature–composition diagram for the system albite–anorthite has stimulated continued discussion among mineralogists and petrologists which, to date, has not produced an adequate graphical or even conceptual treatment of the phase relations. Previously proposed phase diagrams treated the Huttenlocher (An_{66}–An_{87}) and Bøggild (An_{45}–An_{65}) miscibility gaps as conventional solvi (McConnell, 1974a, Fig. 5; Wenk, 1979, Fig. 3). As an alternative, Smith (1972, Fig. 9; 1974, Fig. S-2a) suggested that the Bøggild gap was the result of a first-order $C\bar{1} \rightleftarrows I\bar{1}$ transition while retaining the Huttenlocher gap as a solvus.

We propose an alternative to these *T–X* diagrams which integrates the miscibility gaps and the ordering transitions in calcic plagioclase. Assuming that the $C\bar{1} \rightleftarrows I\bar{1}$ and $I\bar{1} \rightleftarrows P\bar{1}$ transitions in plagioclase are higher than first order, tricritical points may occur in analogy to other well-studied binary systems (Allen and Cahn, 1976a, 1976b). The proposed *T–X* diagram contains two such tricritical points, in

0003–004X/83/0102–0041$02.00

addition to the tricritical point proposed by Carpenter (1981) for the peristerite region. The tricritical points each generate a conditional spinodal (conditional on the appearance of a lower-symmetry ordered phase) as well as a region of stable two-phase coexistence for the ordered and disordered phases.

The paper begins with a summary of the compositions of coexisting plagioclase feldspars in rocks metamorphosed under a range of temperature conditions. Next, we present observations of microstructures in calcic plagioclase made with the transmission electron microscope (TEM). Two possible phase diagrams for the calcic portion of the albite–anorthite system are derived from the information on the compositions and microstructures of plagioclases. Finally, the proposed phase diagrams are used to interpret the variety of microstructures reported in the literature for intermediate and calcic plagioclase feldspars.

Many of the microstructures in plagioclase are interpreted in terms of metastable behavior. This is not unreasonable, because subsolidus reactions in the plagioclase system require the coupled solid state exchange NaSi ⇄ CaAl. Interdiffusion coefficients for the exchange couple may be estimated from the heating experiments of Nord *et al.* (1974) who homogenized the lamellae of Huttenlocher intergrowths by annealing them at high temperatures for short periods of time. Assuming an $x = \sqrt{Dt}$ law for homogenization of lamellae, a diffusion coefficient of $D \sim 10^{-17}$ cm^2/sec at 1240° and 1300°C is calculated. Under conditions of upper amphibolite facies metamorphism ($T \sim 650$°C), Huttenlocher lamellae grow to a thickness of >1000Å (Grove, 1977) and an estimated D would be on the order of 10^{-26} cm^2/sec. These two data allow estimation of the kinetic rate constant and yield an activation energy for coarsening in excess of 420 kJ/mol. Thus, plagioclase reactions that occur by diffusion-controlled NaSi ⇄ CaAl exchange are extremely slow, and the opportunity for the formation of metastable plagioclase compositions in nature is great. Some reaction mechanisms (heterogeneous nucleation) may indeed produce equilibrium phases, while other mechanisms (*e.g.*, spinodal decomposition) may commonly produce metastable feldspars. An important aspect of our proposed *T–X* diagram is that it allows prediction of possible metastable ordering and decomposition mechanisms and hence permits identification of equilibrium *vs.* metastable feldspars in natural occurrences of plagioclase.

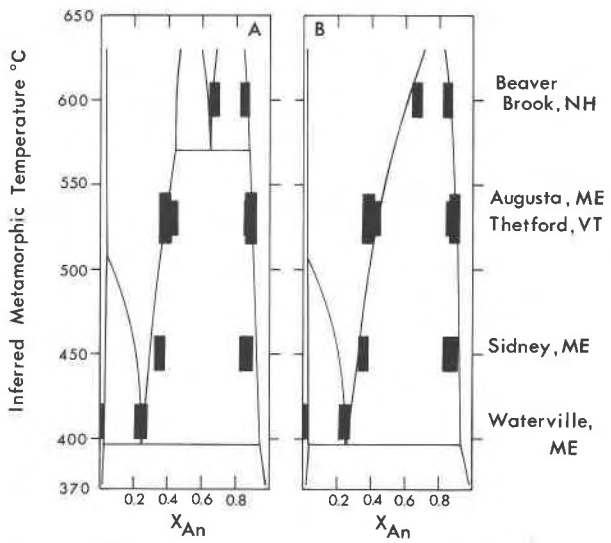

Fig. 1. Electron microprobe analyses of plagioclase from metamorphic rocks. The dark rectangles represent preferred compositions of plagioclase obtained by compiling analyses on histograms and choosing compositions with maximum frequency. Temperatures were estimated using geothermometric techniques. Beaver Brook locality temperature estimate is from Rumble *et al.* (1982). The Thetford, Vermont temperature is found in Spear (1980, 1981). The Augusta (Ferry, 1976), Sidney (Ferry, 1979) and Waterville (Ferry, 1980a) localities are representative of Buchan-type metamorphism in the Waterville-Vassalboro region, South-Central Maine. This technique may show equilibrium compositions, if grains represent plagioclase produced by heterogeneous nucleation. The peristerite gap is drawn as a conditional spinodal (Carpenter, 1981), and the univariant equilibrium at 390°C would involve $P\bar{1}$, $C\bar{1}$ disordered andesine and $C\bar{1}$ ordered albite. (a) This variant treats the Bøggild gap as stable at $T > 575$°C. (b) This topology shows no stable Bøggild gap at high temperatures.

Compositions of plagioclase feldspar in metamorphic rocks

Compositions of coexisting plagioclase feldspars in metamorphic rocks constrain the topology of any proposed *T–X* diagram for the albite–anorthite system. Many feldspars in metamorphic rocks probably formed by heterogeneous nucleation and therefore may represent stable equilibrium phases. Figure 1 summarizes temperature and composition data for coexisting feldspars from metamorphic rocks crystallized under a variety of temperature conditions. Coexisting albite and oligoclase are found in phyllites metamorphosed at $P \sim 3500$ bars, $T = 400° \pm 10$°C near Waterville, Maine (Ferry, 1976, unpublished data). Coexisting albite and oligoclase have long been recognized in low-grade metamorphic rocks (Crawford, 1966; Evans, 1964). Coexisting andesine and bytownite have been reported in carbonate rocks near Sidney, Maine,

metamorphosed at $P \sim 3500$ bars, $T = 450° \pm 10°C$ (Ferry, 1979) and in mafic volcanic rocks near Thetford, Vermont, metamorphosed at $P \sim 5500$ bars, $T = 535° \pm 20°C$ (Spear, 1980, 1981).

The coexisting andesine + bytownite from Thetford, Vermont, is particularly important because Spear demonstrated, on the basis of plagioclase–amphibole cation exchange equilibria, that it indeed represents a stable equilibrium pair. An exchange reaction exists among the albite (NaSi) and anorthite (CaAl) components of plagioclase and the glaucophane ($Na^{M4}Si^{IV}$) and tschermakite ($Ca^{M4}Al^{IV}$) components of calcic amphibole. At Thetford, coexisting andesine (An_{39}) and bytownite (An_{88}) occur with amphibole of a unique composition in terms of glaucophane and tschermakite components (Spear, 1980, Fig. 1). Feldspars more sodic than An_{39} coexist with more sodic (glaucophane-rich) amphiboles. Feldspars more calcic than An_{88} coexist with more calcic (tschermakite-rich) amphiboles. The systematic NaSi $\rightleftarrows$ CaAl partitioning among phases at Thetford, Vermont, is strong evidence that coexisting An_{39} and An_{88} represent a stable equilibrium assemblage. In fact, any supposed two-plagioclase pair must be consistent with mineral equilibria involving coexisting phases, if the pair is to be treated seriously as an equilibrium assemblage.

The plagioclase feldspars in samples from Thetford, however, do exhibit some complications. In thin section the coexisting andesine and bytownite are usually present as patchy mutual intergrowths or as bytownite overgrowths on andesine cores. The overgrowth relation is consistent with the production of $CaAl_2Si_2O_8$ by prograde mineral reactions. The sodic plagioclases acted as nucleii on which heterogeneous nucleation of an equilibrium calcic plagioclase occurred. Detailed examination of the coexisting andesine and bytownite reveals that the andesine cores are optically homogeneous, but are continuously zoned from An_{30} to An_{39}. Occasionally there is an abrupt transition from An_{39} to an An_{88} bytownite rim. Commonly, there are regions of optically visible two-phase intergrowths between the andesine core and bytownite rim which range in bulk composition from An_{69} to An_{86} (Fig. 2). The two-phase lamellar intergrowths grade outward into optically homogeneous An_{88} bytownite. As discussed further below, we interpret the coexisting An_{39} + An_{88} as a stable equilibrium pair and the lamellar intergrowths as a metastable phenomenon.

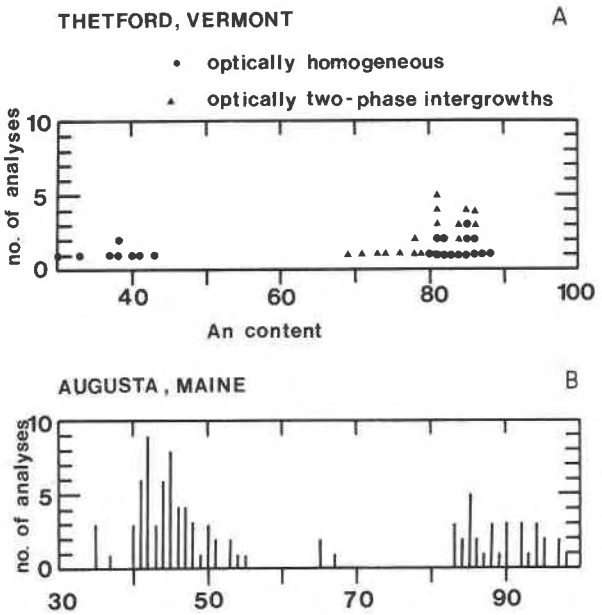

Fig. 2. Histograms of electron microprobe analyses of plagioclase from metamorphic rocks. (a) Thetford, Vermont. Closed circles are analyses of areas which appear to be a homogeneous single phase under the optical microscope. Triangles are bulk analyses of optically visible two phase intergrowths. (b) Augusta, Maine. A compilation of analyses from outcrop 987 (Ferry, 1980a).

Coexisting andesine and bytownite are also inferred to occur at temperatures ~530°C ($P \sim 3500$ bars) based on the study of a large single outcrop of metamorphosed carbonate rock near Augusta, Maine (location 987 of Ferry, 1980a). Figure 2 summarizes compositions of plagioclase found in 22 samples from the outcrop. Although no rock contained coexisting andesine and bytownite, analyses demonstrate that compositions of ~An_{40} and ~An_{90} are strongly favored. The activity of anorthite was calculated for plagioclase in each sample by the following procedure. First, using samples that contain plagioclase of composition $X_{An} \geq 0.9$, the temperature of metamorphism at the outcrop was calculated from the assemblages plagioclase + calcite + zoisite + calcic amphibole + quartz + diopside and plagioclase + calcite + zoisite + quartz + garnet. Calculations followed a scheme outlined earlier (Ferry, 1976), modified by using thermochemical data for the zoisite–calcite–anorthite equilibrium extracted from recent experiments by Allen and Fawcett (1982). Conditions of $P_{CO_2} + P_{H_2O} = P_{total} = 3500$ bars were assumed. Only those samples containing plagioclase of $X_{An} \geq 0.9$ were used in calculations of temperatures because for these samples $a_{An} \sim X_{An}$ (Orville, 1972; Goldsmith,

Table 1. Calculated activity of anorthite component in plagioclase for samples collected from a single outcrop of amphibolite facies metamorphosed carbonate rock

Sample	X_{An}	A_{An}^{1}	A_{An}^{2}
A	0.88–0.94	0.89–0.94	1.04–1.34
B	0.90–0.93	0.90–0.93	0.82–0.97
C	0.43–0.65	0.55–0.76	0.86–0.96
D	0.42–0.44	0.54–0.56	0.95–1.41
E	0.85–0.88	0.87–0.89	1.10–1.29
F	0.83–0.85	0.85–0.87	1.16–1.30
G	0.35–0.37	0.45–0.47	0.92–1.01*
H	0.44–0.46	0.56–0.59	1.01–1.20
I	0.42–0.45	0.54–0.57	0.81–0.94
K	0.68–0.86	0.77–0.87	1.06–1.22
L	0.49–0.51	0.63–0.65	0.97–1.25
M	0.40–0.43	0.51–0.55	0.92–1.06
N	0.41–0.47	0.52–0.60	0.92–1.01
P	0.84–0.87	0.86–0.88	0.90–1.05
Q	0.48–0.50	0.61–0.64	0.87–0.99
R	0.40–0.45	0.51–0.57	0.86–0.89
S	0.41–0.47	0.52–0.60	0.89–1.02
T	0.92–0.95	0.92–0.95	0.81–0.92, 0.92–1.22*
W	0.40–0.42	0.51–0.54	0.80–0.91*
X	0.96–0.98	0.97–0.98	0.95–1.27
987I	0.83–0.86	0.85–0.87	0.87–1.12
987II	0.94–0.95	0.94–0.95	0.84–1.24

[1] Calculated from activity coefficients of Orville (1972).

[2] Calculated by method described in text using diopside–calcite–amphibole–quartz–fluid equilibrium except where noted by *).

* activity calculated from plagioclase–garnet–quartz–zoisite equilibrium.

1982). Temperature so calculated from five samples is consistent with 530°±10°C. The 530°C temperature is confirmed by results of a regional study of metamorphic temperatures in an area immediately adjacent to the outcrop (Ferry, 1980b). Second, for all 22 samples the equilibrium composition of coexisting H_2O–CO_2 fluid was calculated at P = 3500 bars, T = 530°C using either the amphibole–calcite–quartz–diopside–fluid or the zoisite–calcite–quartz–garnet–fluid equilibrium. Third, the activity of anorthite in each sample was determined from the zoisite–plagioclase–calcite–fluid equilibrium at conditions of P = 3500 bars, T = 530°C, and X_{CO_2} as previously determined. Results are presented in Table 1. The range in calculated activities is that permitted by the range in measured mineral compositions in the assemblages zoisite–quartz–calcite–garnet and zoisite–quartz–calcite–amphibole–diopside. For comparison, the composition of plagioclase in each sample is listed as well as the activity of anorthite that would be calculated from the activity coefficients of Orville (1972). For twelve samples in which X_{An} = 0.35–0.51, the mean a_{An} = 0.97 (σ = 0.10). Mineral equilibria indicate that plagioclase of composition $X_{An} \sim 0.4$–0.5 behaved chemically as if it were equivalent to plagioclase of composition $X_{An} \sim 0.9$–1.0 during the metamorphic event. Calculated activities (Table 1), combined with the clustering of observed compositions (Fig. 2), are interpreted in terms of a miscibility gap between $\sim An_{40}$ and $\sim An_{90}$ at the physical conditions of metamorphism (530°C).

Figure 2, however, reveals complications similar to those observed in the sample from Thetford, Vermont. Although a stable two-phase region is inferred between $\sim An_{40}$ and $\sim An_{90}$, compositions have been observed that lie within the proposed miscibility gap. We believe these intermediate compositions represent metastability and will discuss them fully in a later section.

Coexisting labradorite and bytownite were observed in carbonate rocks metamorphosed at $P \sim$ 3500 bars, T = 600°±10°C from Beaver Brook, New Hampshire. Coexisting $\sim An_{65}$ and $\sim An_{85}$ have been reported in metamorphic rocks from a number of other localities (*e.g.*, Wenk and Wenk, 1977).

Two interpretations of the observed plagioclase compositions in metamorphic rocks are presented in Figure 1. Above 575°C either there may exist a single two-phase region representing coexisting labradorite and bytownite or there may exist two two-phase regions, one for coexisting labradorite and bytownite and the other for coexisting andesine and labradorite. Existing data force us to adopt both as possible valid phase diagrams. Figure 1a obviously would be preferred if a stable equilibrium coexistence between andesine and labradorite could ever be demonstrated.

TEM observations of metamorphic plagioclase

Thetford, Vermont

Samples of the two plagioclase assemblage from Thetford, Vermont were chosen for TEM observation. Thin sections polished on one side were prepared using Crystalbond and areas were selected for TEM examination. The thin sections were mounted between 3 mm diameter Cu grids with epoxy, and an ion micro-milling device was used to thin the sample. Observations were made with a Phillips EM300 TEM operating at 100 kV. In order to relate the observed microstructures and diffraction geometry to bulk chemical composition, thin regions of interest were semi-quantitatively analyzed on an electron microprobe using energy dispersive techniques.

Bytownite (An_{87-89}) appears to be a single phase when viewed with the optical microscope. Selected area diffraction patterns show that this composition has the ordered anorthite structure. Weak-diffuse *c* and *d* reflections reveal the presence of domains with $P\bar{1}$ symmetry (Fig. 3a). Dark field observations made using the *b* reflections ($h + k$ = odd, l = odd) characteristic of the $I\bar{1}$ ordered structure show (Fig. 4a) zig-zag *b* antiphase boundaries (APBs) that separate ordered domains.

TEM observation of regions containing optically visible two-feldspar intergrowths show characteristics identical to those of Huttenlocher intergrowths (Nissen, 1968, 1974; McLaren, 1974; McConnell, 1974a; Grove, 1976). Selected area diffraction patterns (Fig. 3b) show that the two-phase intergrowths consist of coexisting $P\bar{1}$ ordered bytownite and labradorite with the periodic antiphase structure of intermediate plagioclase. In calcic bulk compositions (Fig. 4b) the bytownite phase predominates and lamellae of intermediate plagioclase show a continuous variation in orientation and spacing of the periodic APBs. The variation in orientation and spacing is consistent with compositional variation in the labradorite phase from An_{66} to An_{75} (Bown and Gay, 1958). Dark field images made with $P\bar{1}$ diffractions reveal $P\bar{1}$ antiphase domains (APDs) elongate parallel to (010) and 30 to 60Å in width (Fig. 4c). In two-phase intergrowths of sodic bulk compositions the labradorite (An_{66}) phase predominates (Fig. 5), and it contains bytownite lamellae. The bytownite lamellae, in turn, contain lamellae of intermediate plagioclase which have periodic APBs that show continuous variations in periodicity and orientation. A similar variation was observed in other Huttenlocher intergrowths (Cliff *et al.*, 1976; Grove 1976, 1977). The bulk composition of the two-phase intergrowths (Fig. 2), their diffraction geometry (Fig. 3b), and the periodic APB morphology all indicate that the lamellae are members of the Huttenlocher miscibility gap (An_{66}–An_{87}).

Regions of Huttenlocher intergrowths are in direct contact with andesine (Fig. 4d), which has the periodic antiphase structure. Sometimes a plagioclase grain contains patches of single-phase andesine surrounded by regions of Huttenlocher intergrowths, and such textural relations are also visible in the optical microscope. Selected area diffraction patterns of andesine lack *f* diffractions, and show diffuse, weak *e* superlattice spots characteristic of the An_{40} periodic antiphase structure (Fig. 3c) with orientation and spacing identical to those of andesine measured by Bown and Gay (1958). In the (100) projection the periodic APB orientation (Slimming, 1976) is nearly parallel to c^* and the splitting

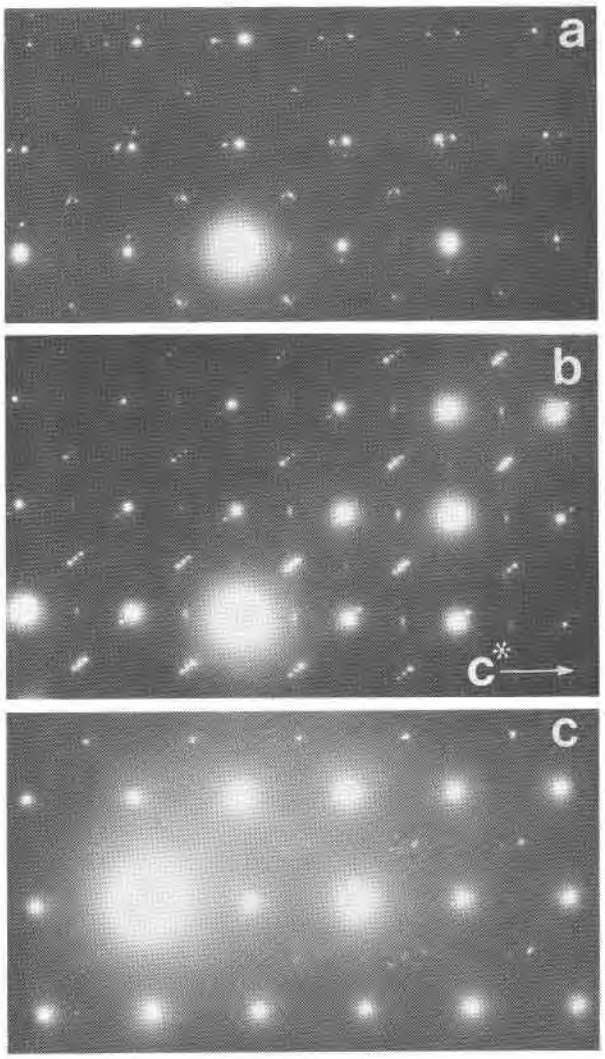

Fig. 3. Selected area diffraction patterns of the [100] pole of Thetford plagioclases. c^* is horizontal and b^* is vertical. See Ribbe (1975, Fig. R-40) for plagioclase diffraction pattern nomenclature. (a) Bytownite (An_{87}) shows $P\bar{1}$ diffraction symmetry. Streaks on *b* reflections arise from *e* plagioclase precipitates that have nucleated on *b* APBs. Specimen shows albite and pericline twinning. (b) Huttenlocher intergrowths with diffraction geometry characteristic of coexisting $P\bar{1}$ (An_{87}) and intermediate plagioclase (An_{66}). The $P\bar{1}$ phase has sharp *b* and diffuse *c* and *d* diffractions and the intermediate plagioclase phase is identified by *e* satellites. The maximum intensity of the *e* satellites occurs at a reciprocal lattice position characteristic of An_{66}. The curved streak connecting *e*–*b* is caused by variable periodicity and orientation of intermediate plagioclase APBs within the intergrowth. (c) Andesine diffraction geometry shows weak *e* satellites with orientation and spacing indicative of An_{40}.

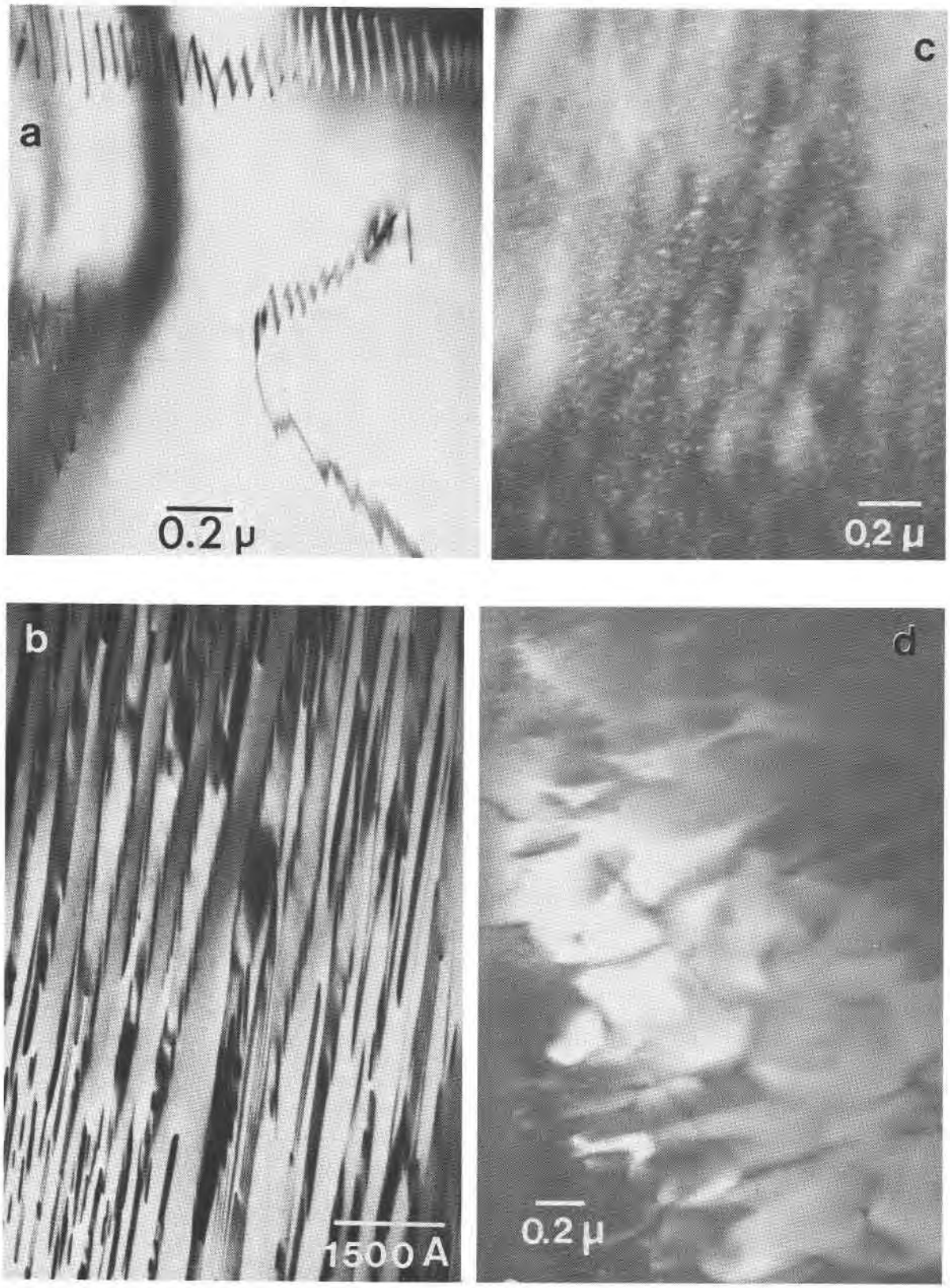
a
0.2 μ
c
0.2 μ
b
1500 A
d
0.2 μ

magnitude is $0.036Å^{-1}$ or 28Å. All features are characterisitc of andesine intermediate plagioclase. Conversely, the periodicity and orientation of *e* satellites in the Huttenlocher intergrowths (Fig. 3b) are identical to those measured in An_{66} to An_{75} labradorite (Bown and Gay, 1958; Grove, 1977).

Dark field micrographs taken in the andesine regions using *e* reflections show a mottled contrast (Fig. 4d), which indicates that the periodic APB structure is coherent over small areas of <1000Å and may be separated by regions of $C\bar{1}$. The diffuseness of *e* spots in selected area diffraction patterns is further evidence of the presence of *e* domains with short-range order and, as a consequence, it is difficult to obtain superlattice images of the periodic APBs.

Augusta, Maine

Samples of An_{50} labradorite from 987-L appeared to be a single phase when viewed with the optical microscope, and were chosen for TEM study. Selected area diffraction patterns (Fig. 6a) contain, in addition to *a* diffractions, sharp *e* and *f* superlattice diffractions with orientation and spacing characteristic of those measured in An_{50} labradorite by Bown and Gay (1958).

Dark field images using *e* diffractions (Fig. 6b) show a domain texture with a weak, mottled contrast. McLaren and Marshall (1974) observed similar domains in a Lake County labradorite, and interpreted the boundaries between domains to be regions of $C\bar{1}$ structure. The texture in the Augusta labradorite consists of domains of coherent periodic antiphase structure separated by boundaries of $C\bar{1}$ structure. Similar periodic APB morphologies were observed by Wenk and Nakajima (1980, Fig. 2a) in an igneous labradorite.

Tricritical Points: theory and application to calcic plagioclase feldspars

The phase transitions that occur in the calcic portion of the plagioclase binary ($C\bar{1} \rightleftarrows I\bar{1}$ and $I\bar{1} \rightleftarrows P\bar{1}$) were inferred by X-ray crystallographers (Laves and Goldsmith, 1951; Gay, 1953) through observation of variable Bragg diffraction morphology. Some plagioclases were found to contain weak, diffuse *b* reflections ($h + k$ = odd, l = odd), suggestive of a transition from a $C\bar{1}$, c = 7Å disordered form to an ordered $I\bar{1}$, c = 14Å modification. Further ordering led to the $P\bar{1}$, c = 14Å structure, and Bragg reflections associated with this space group (*c* and *d* diffractions, with $h + k$ = even, l = odd or $h + k$ = odd, l = even) had a morphology distinct from other diffractions, indicating the presence of short-range ordered domains with this lowest symmetry. The existence of two types of APDs and the presence of two order/disorder transitions were further substantiated by direct observation of both types of domains in the TEM (McLaren and Marshall, 1974; Heuer and Nord, 1976).

Thus, in the calcic portion of the plagioclase system there exist three structural modifications, and the transformation sequence for a phase of fixed composition, from high to low temperature, is:

$$C\bar{1} \rightarrow I\bar{1} \rightarrow P\bar{1}$$

The lower symmetry structures are derived from their higher symmetry precursors through the loss of a translational operation, which reduces the number of inversion centers in the triclinic cell by half. The consequence of the transformation from $C\bar{1}$ to $I\bar{1}$ is a doubling of the *c* axis or the loss of the 1/2 [110] translation. Similarly, the $I\bar{1}$ to $P\bar{1}$ transition results in the loss of the 1/2 [111] translation.

Transitions involving ordering and atomic position displacements may qualify as higher order (Landau and Lifshitz, 1958). In the case of the $C\bar{1} \rightleftarrows I\bar{1}$ transition, a continuously varying set of Al–Si tetrahedral site occupancies probably exists between the ordered $I\bar{1}$ and disordered $C\bar{1}$ states. For the $I\bar{1} \rightleftarrows P\bar{1}$ transition, there appear to be both

Fig. 4. TEM observations of Thetford plagioclase. (a) Dark field (DF) electron micrograph of bytownite (An_{87}) shows zigzag *b* APBs; *g* (reciprocal lattice vector) = 031. The APB orientations parallel the Huttenlocher exsolution interfacial orientation ($03\bar{1}$) and the orientation of the An_{75} periodic antiphase structure ($01\bar{1}$). (b) Huttenlocher intergrowths in bytownite ($\sim An_{82}$). A *b* diffraction and its surrounding *e* satellites were used to form this dark field image. Labradorite plagioclase ordered on the periodic antiphase structure is intergrown with a $P\bar{1}$ calcic phase. The periodic APBs extend into the calcic regions as isolated boundaries and as single periodic antiphase domains. Note variation in orientation and periodicity of periodic APBs in labradorite. This variation is equivalent to that observed over the compositional range An_{66} to An_{75}. DF, $g = 0\bar{1}5$ near [100]. (c) Elongate fine scale *c* APDs in the $P\bar{1}$ bytownite phase of a Huttenlocher intergrowth. Some contrast from the labradorite lamellae shows the interphase boundaries to be nearly vertical in this photo. DF, g = 005 (d) contrast from an *e* reflection in a region of An_{40} andesine. The mottled texture results from the growth of domains ordered on the periodic antiphase structure, and is typical of textures in which decomposition to metastable $C\bar{1}$ and $I\bar{1}$ (periodic antiphase) has occurred within the Bøggild conditional spinodal DF, g = 031.

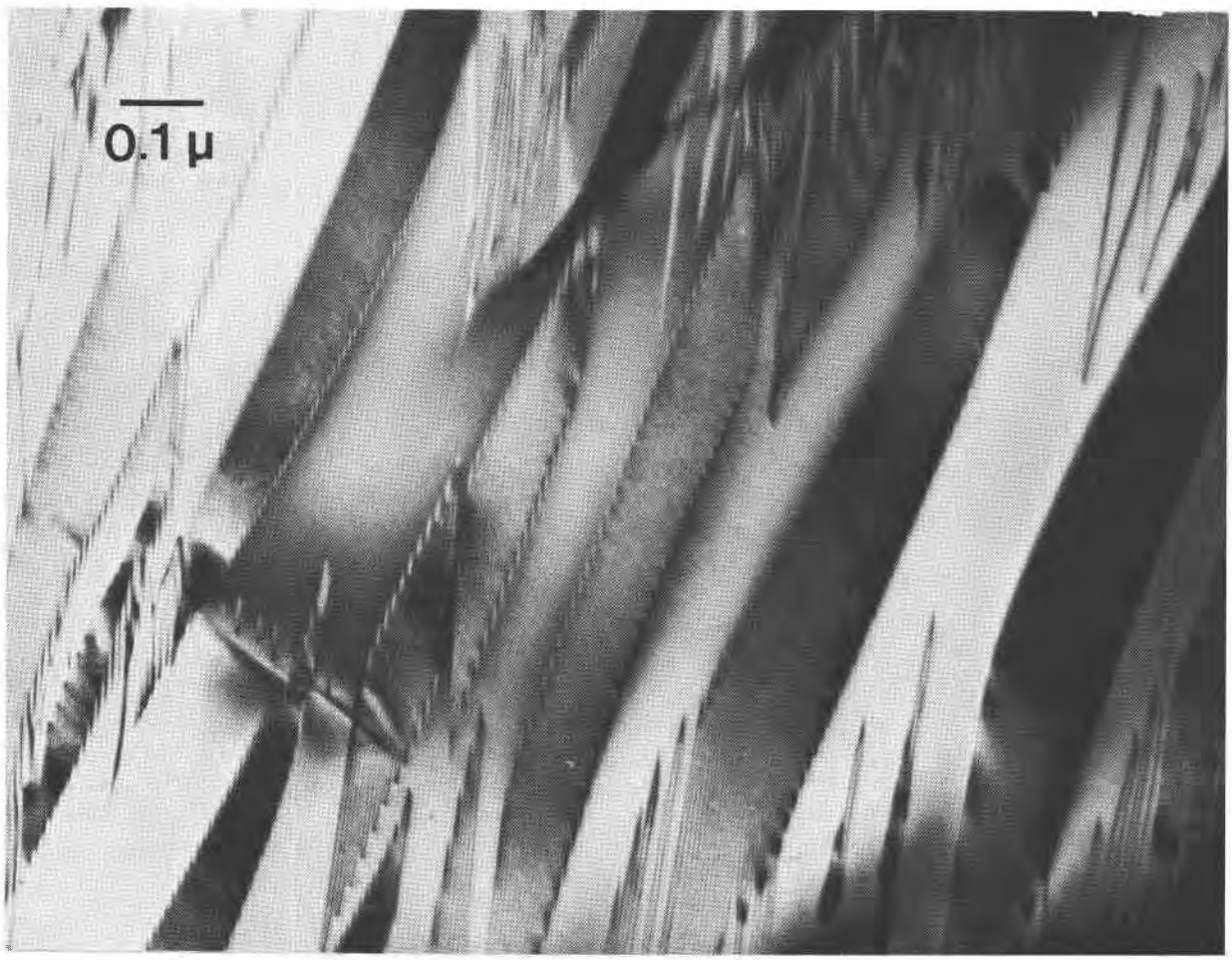

Fig. 5. Huttenlocher intergrowths in Thetford labradorite ($\sim An_{71}$). DF, $g = 031$. This region was adjacent to bytownite in Fig. 3a.

atomic position (displacive) and Al–Si site occupancy contributions to the transition. Thus, both $C\bar{1} \rightleftarrows I\bar{1}$ and $I\bar{1} \rightleftarrows P\bar{1}$ may be higher order transitions. For second order or higher order transitions there is a continuous change in the physical properties of the phase up to the transition, where it acquires a new symmetry property. State functions vary continuously through the transition. The free energy at the phase transition point has a singularity; the derivatives with respect to intensive parameters (*e.g.* $\partial G/\partial X$) are continuous, but the second derivatives of free energy with respect to intensive variables are discontinuous. In one direction along the composition coordinates from the transition point on a *G–X* diagram there are two free energy *vs.* composition curves: one for the ordered and another for the disordered phase (Fig. 7a). In the other direction along the composition coordinate from the transition point the *G*-curve for the ordered phase does not exist. For transitions of this type the degree of order in the ordered phase changes continuously with composition up to the transition and an ordering parameter (η) may be used to describe the differences. As the transition point is approached η changes continuously. At the transition temperature $\eta = 0$, the symmetry increases and a free energy curve for the lower symmetry phase no longer exists.

When phase transitions are second order or higher, tricritical points and conditional spinodals may exist under some conditions (Allen and Cahn, 1976a,b; Allen, 1977). At a tricritical point $\partial^2 G/\partial X^2 = 0$ for the lower symmetry phase (Fig. 7b), and at temperatures below the tricritical point $\partial^2 G/\partial X^2 < 0$ for a range of composition (Fig. 7c). Thus, a miscibility gap develops between the ordered and disordered phases (Fig. 7d) which is conditional on the presence of the ordered phase. Within the miscibil-

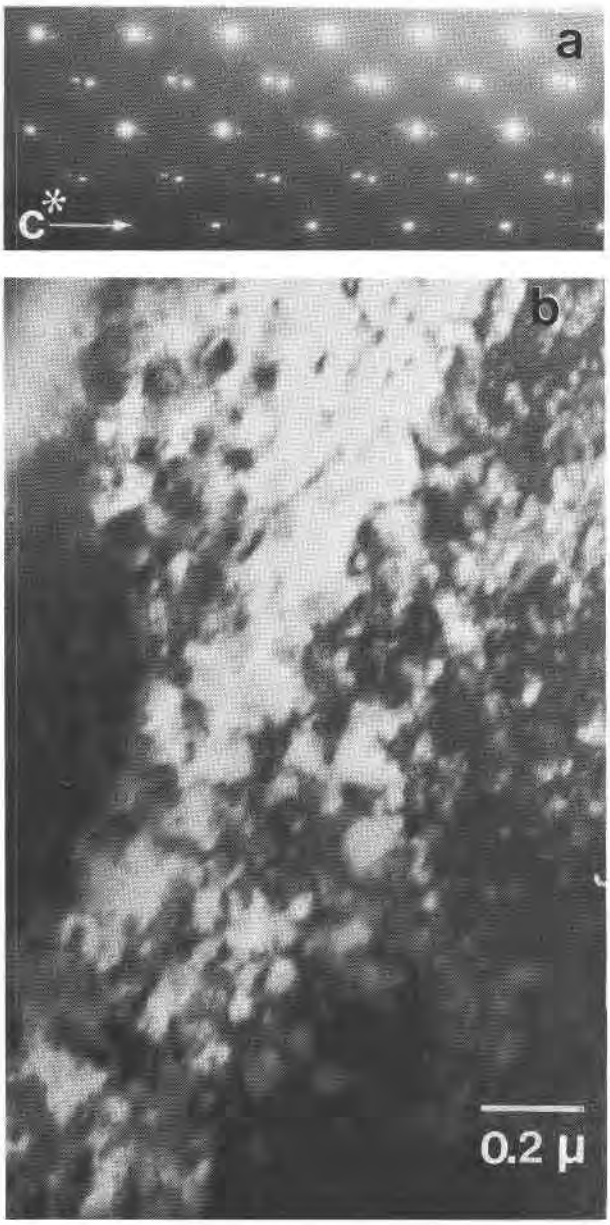

Fig. 6. (a) Selected area diffraction pattern of the [100] pole of Augusta An_{50} plagioclase. c^* is horizontal and b^* is vertical. The diffraction geometry is characteristic of An_{50} intermediate plagioclase. (b) Dark field electron micrograph of Augusta labradorite (An_{50}) taken with an e reflection. The domain-like contrast results from the following transition sequence. $C\bar{1}$ labradorite orders to $I\bar{1}$ and APBs are formed. Spinodal decomposition to $C\bar{1}$ + $I\bar{1}$ within the Bøggild conditional spinodal follows with the $C\bar{1}$ phase forming at the antiphase boundaries.

ity gap a spinodal is defined on one side by the metastable extension of the order-disorder transition (where the slope of the G–X curve changes from positive to negative) and on the ordered side by the loci of points for which $\partial^2 G/\partial X^2 = 0$ (Fig. 7d). Within the spinodal region a phase will be unstable with respect to any small change in composition and spinodal decomposition may occur.

In a system with a tricritical point, phase separation within the conditional spinodal requires the presence of the ordered phase. Consider a composition in Figure 7d which lies in the disordered (α) phase region and that will cross the metastable

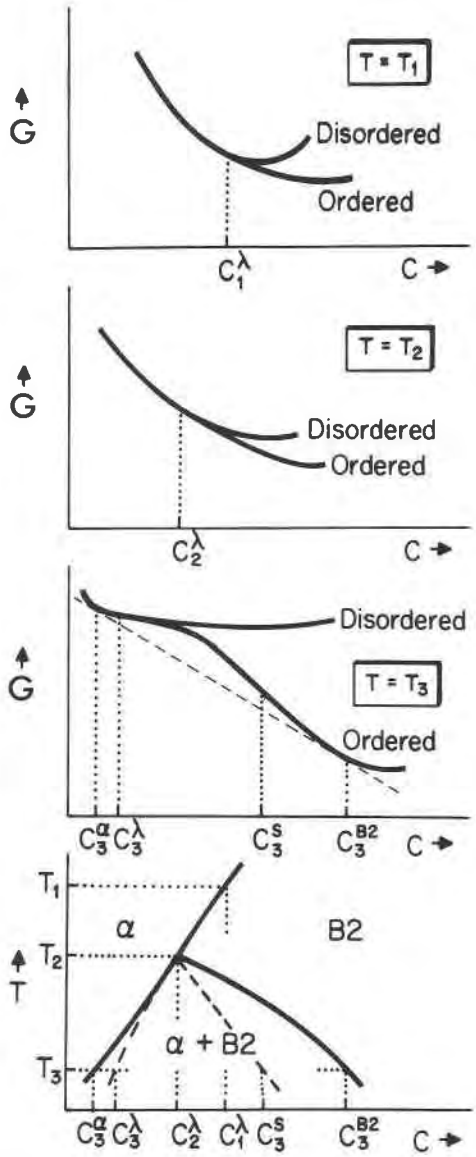

Fig. 7. Free energy (G)-composition (c) diagrams are used to construct a temperature–composition diagram of a tricritical point. Free energy surfaces are constructed for 3 temperatures: T_1 is above the tricritical point; T_2 is at the tricritical point; and T_3 is below the tricritical point within the miscibility gap. From Allen and Cahn (1976a).

extension of the line of the higher order transition on cooling. For this composition ordering must precede phase separation, and domain size and morphology will influence the resultant decomposition texture. A composition initially in the B2 field will undergo decomposition within the conditional spinodal to α + B2 (Fig. 7d). As discussed by Allen and Cahn (1976a) the relative energies of APBs and the interface between the ordered and disordered phases become equivalent and vanish at the tricritical point. As an order–disorder transition is approached from the lower symmetry phase, the APBs, which are present as a consequence of the lower symmetry, will disappear, and the interfacial energy approaches zero. The phase boundary energy for the interface between ordered and disordered phases in the vicinity of the tricritical point will also tend to zero. As a consequence, the higher symmetry phase will wet APBs in the ordered phase. If small ordered domains with dimensions of the spinodal wavelength are present, the disordered phase will form at the APBs, where η approaches zero. If domains are large, spinodal decomposition will occur within the ordered regions and will have its characteristic wavelength and orientation.

In their study of Fe–Al alloys, Allen and Cahn (1976a) provided a theoretical framework for the representation of phase changes near tricritical points and applied it to ordering and decomposition phenomena in the system Fe–Al. There are two ordering reactions in Fe–Al: one involves the transition from α (*Im*3*m*, disordered FeAl) to B2 (*Pm*3*m*, ordered FeAl). A second ordering transition involves B2 $\rightleftarrows$ DO_3 (*Fm*3*m*, ordered Fe_3Al). There is a symmetrical tricritical point associated with the $\alpha \rightleftarrows$ B2 transition (Fig. 7d) and a metastable tricritical point associated with the B2 $\rightleftarrows$ DO_3 transition. The three structural modifications are related by higher order transitions which proceed through the loss of a translational symmetry operation. The transition sequence $\alpha \rightarrow$ B2 $\rightarrow$ DO_3 thus is directly analogous to the $C\bar{1} \rightarrow I\bar{1} \rightarrow P\bar{1}$ transition sequence in calcic plagioclase because both involve the loss of half the inversion centers in the lower symmetry form.

Carpenter (1981) has suggested the existence of a tricritical point associated with the peristerite gap in the system $NaAlSi_3O_8$–$CaAl_2Si_2O_8$. Because of the analogy between the order–disorder transition sequence $\alpha \rightarrow$ B2 $\rightarrow$ DO_3 in the system Fe–Al and the transition sequence $C\bar{1} \rightarrow I\bar{1} \rightarrow P\bar{1}$ in the system $NaAlSi_3O_8$–$CaAl_2Si_2O_8$, we propose that two additional tricritical points occur in the calcic portion of the albite–anorthite system. One tricritical point is stable and associated with the $C\bar{1} \rightleftarrows I\bar{1}$ transition. The other tricritical point is associated with the $I\bar{1} \rightleftarrows P\bar{1}$ transition and may be either metastable (as in Fe–Al) or stable. In the remainder of the paper we will explore the application of tricritical phenomena to the calcic portion of the system $NaAlSi_3O_8$–$CaAl_2Si_2O_8$. We will derive a model subsolidus *T-X* phase diagram for the plagioclase system and develop predictions of phase transition/exsolution sequences and limits of metastability. Finally, we will discuss the voluminous TEM observations of plagioclase microstructures in light of our model phase diagram.

A phase diagram for the calcic, subsolidus portion of the system $NaAlSi_3O_8$–$CaAl_2Si_2O_8$

Location of $C\bar{1} \rightleftarrows I\bar{1}$ and $\rightleftarrows P\bar{1}$ transitions in T–X space

Although there is some uncertainty as to the precise temperatures of the $C\bar{1} \rightarrow I\bar{1}$ and $I\bar{1} \rightarrow P\bar{1}$ transitions in anorthite, single crystal X-ray structure refinements performed at elevated temperatures and heating stage observations of APBs made with the TEM may be used to infer the transition temperatures. Similarly, the temperature–composition path traced by these transitions into the binary system and the positions of the tricritical points can be inferred from TEM observations of natural samples.

The $C\bar{1} \rightleftarrows I\bar{1}$ transition. McLaren and Marshall (1974) synthesized anorthite near its melting temperature (1530°C), cooled the sample to 1400°C and annealed it for 8 days. The sample was examined in the TEM and found to contain *b* APDs ~ 0.2 microns wide arising from the $C\bar{1}$ to $I\bar{1}$ ordering transition. Single-crystal X-ray structure refinements of anorthite performed at elevated temperatures have been carried out at 400° and 830°C by Foit and Peacor (1973), at 250°C and 1430°C by Czank (1973), and at room temperature on an anorthite annealed at 1530°C for 30 minutes (Bruno *et al.*, 1976). In all cases the diffraction symmetry was $I\bar{1}$ and the results of structure refinements were compatible with the presence of $I\bar{1}$ order. These observations indicate that the $C\bar{1}$ to $I\bar{1}$ transition occurs above 1430°C for anorthite. The TEM observations of Nord *et al.* (1973) provide a point in composition–temperature space for the $C\bar{1}$ to $I\bar{1}$ transition. In compositionally zoned plagioclase (~An_{90}) from the groundmass of lunar breccia

60335, Nord *et al.* found the transition from a region of single-domain $I\bar{1}$ to multi-domain $I\bar{1}$, indicating that this plagioclase passed through the $C\bar{1} \rightleftarrows I\bar{1}$ transition as it crystallized from the melt. The experimental results of Walker *et al.* (1973) determined that the groundmass crystallization temperature and hence the $C\bar{1} \rightleftarrows I\bar{1}$ transition temperature for 60335 was ~1275° to 1225°C (Figs. 8 and 9a).

The $I\bar{1} \rightleftarrows P\bar{1}$ transition. Several investigators (summarized by Heuer *et al.*, 1976) have used heating stage experiments in the TEM to determine the temperature of the $I\bar{1} \rightleftarrows P\bar{1}$ transition in anorthite. They found that the diffractions characteristic of the $P\bar{1}$ space group and the domain contrast became weak at 200° to 250°C, but that the domain morphology reappeared unchanged after cooling. This behavior persisted up to the highest temperature studied (575°C) by Müller and Wenk (1973) and to a temperature between 400° and 623°C in an anorthite studied by Lally *et al.* (1972). Only after prolonged heating at higher temperatures were the $P\bar{1}$ domains destroyed. Müller and Wenk found that irreversible changes in domain morphology occurred between 575° and 1200°C. Moreover, the high-temperature, single-crystal X-ray structure refinements of Foit and Peacor (1973) indicated that An_{98} plagioclase has the primitive anorthite structure at 830°C, despite the weak intensities of the $P\bar{1}$ diffractions. Heating experiments on An_{98} by Foit and Peacor (1967) determined the temperature of the $I\bar{1}$ to $P\bar{1}$ transition at 1000°C. Differences in the degree of order in the anorthites studied, as well as compositional variability have affected the transition temperature. It is inferred that the transition in

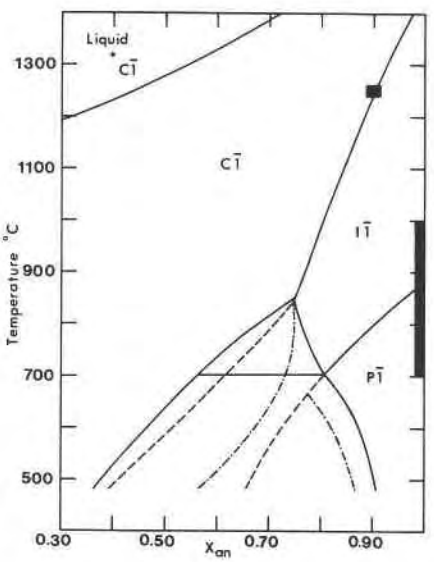

Fig. 8. Proposed temperature–composition diagram for the calcic portion of the system anorthite-albite. Temperature of the $C\bar{1} \rightleftarrows I1$ transition for An_{90} is inferred from TEM observations of Nord *et al.* 1973. The temperature of the $I\bar{1} \rightleftarrows P1$ transition is uncertain and may lie within the range of temperatures (1000°–700°C). Dashed lines are metastable extensions of the higher-order transitions within the miscibility gaps. Dash–dot lines are the traces of the spinodals on the free energy curve of the low symmetry phases. The positions and temperatures of the tricritical points are inferred from TEM observations.

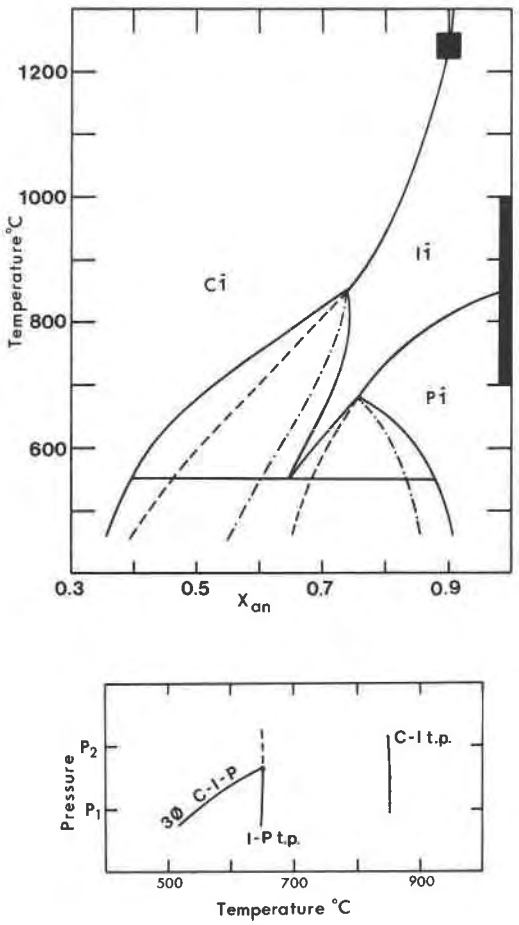

Fig. 9. (a) A possible topology of the temperature–composition diagram for the calcic portion of the system albite–anorthite. This version contains a region of stability for the $I\bar{1}$–$P\bar{1}$ conditional spinodal. Compare with Fig. 8. (b) Pressure–temperature relations for the univariant equilibrium $P\bar{1} + I\bar{1} + C\bar{1}$ (3ϕC–I–P) and the two tricritical points; $C\bar{1}$–$I\bar{1}$ (C–I t.p.) and $I\bar{1}$–$P\bar{1}$ (I–P t.p.). The *T–X* diagram above corresponds to an isobaric section at P_1. The *T–X* diagram in Fig. 8 would correspond to an isobaric section at P_2, a pressure above the invariant point terminal to the $C\bar{1}$–$I1$–$P\bar{1}$ univariant reaction. The $I\bar{1}$–$P\bar{1}$ tricritical point is metastable under these conditions. Temperatures are approximate and pressure increases from P_1 to P_2.

An_{100} lies between 1000°C and 700°C (Figs. 8 and 9a).

Modulated structure of intermediate plagioclase

The periodic antiphase structure characteristic of An_{33} to An_{75} plagioclase will be treated as a thermodynamically stable phase which has ordered with the $I\bar{1}$ structure. A minimization of free energy is attained by transforming from a $C\bar{1}$ disordered form to the $I\bar{1}$ ordered structure, and an accompanying minimization of lattice strains is produced by ordering on a periodic antiphase structure. Structural distortions are associated with Al–Si ordering and the periodic antiphase structure compensates for the overall strain by reversing the distortions at every APB. Fleet (1981) has rationalized the compositional dependence of the orientation of the periodic antiphase boundary by calculating the crystallographic orientations for which dimensional misfit and coherent elastic strain energy of ordered anorthite and disordered albite structures are minimized. The periodic APB represents the best fit between antiordered $I\bar{1}$ domains for a particular composition. McConnell (1978) envisions periodic antiphasing as a structural resonance in which the interactions between ordering and displacements of the appropriate symmetry (the displacement on the APB is the translational operation 1/2 [110]) interact to minimize free energy. Although these two views of the intermediate plagioclase structure differ in several important respects, both involve the generation of $I\bar{1}$ domains. We wish to emphasize the $I\bar{1}$-like characteristics of this structural form and treat it as an antiphased variant. Whether or not it is a spinodally unmixed modulation (Fleet, 1981), or a compositionally homogeneous ordered structure (Korekawa *et al.*, 1978) is a question that is not resolved in this study.

The periodic antiphase structure may be produced through at least two mechanisms. (1) Plagioclase with $C\bar{1}$ symmetry orders to $I1$. Continued ordering in the $I\bar{1}$ domains occur and the thermodynamically stable form is the modulated intermediate plagioclase structure. TEM microstructures characteristic of this transition would be the existence of many small domains (<1000Å in size) which contain the periodic antiphase structure. (2) Spinodal decomposition of preexisting $I\bar{1}$ plagioclase into two compositionally distinct phases may result in the formation of an $I\bar{1}$-ordered phase with periodic antiphase structure. Upon decomposition the reorganization of bonds in the Na-rich phase requires solid state diffusion over large distances, and an $I\bar{1}$ structure with periodic APBs forms as the stable phase. TEM microstructures characteristic of this transition variant would be oriented intergrowths of an Na-rich periodic antiphase structure phase and a Ca-rich ordered phase.

Location of the tricritical points in T–X space

Compositionally zoned plagioclases grow during fractional crystallization of basaltic liquids and provide a continuously varying medium which records subsequent ordering and decomposition sequences. Thus, textural variations in a single zoned feldspar crystal can be used to infer transition and decomposition reactions. Microstructures observed in plagioclase from the Ardnamurchan and Nain intrusives (Grove, 1977) the Stillwater complex (Nord *et al.*, 1974) and from Lake County, Oregon (McLaren and Marshall, 1974; Wenk *et al.*, 1980) will be used in the following discussion to locate the tricritical points in temperature–composition space.

The tricritical point associated with the $C\bar{1} \rightleftarrows I\bar{1}$ transition. Examples of decomposition which was preceeded by ordering below the metastable extension of the $C\bar{1} \rightarrow I\bar{1}$ transition are found in labradorites from volcanic and plutonic environments. McLaren and Marshall (1974, Fig. 2) and Wenk *et al.* (1980) noted a domain texture in Lake County labradorite of $I\bar{1}$ and $C\bar{1}$. Similar domain morphology is found in Ardnamurchan plagioclase (An_{68-74}, Grove, 1977, Fig. 5). These morphologies are produced when plagioclase that is initially $C\bar{1}$ is cooled into the conditional spinodal. Ordering to $I\bar{1}$ occurs below the metastable extension of the $C\bar{1} \rightarrow I\bar{1}$ line and fine scale APDs (~100 to 200Å in width) are formed. Subsequent decomposition of the disordered phase occurs on the APBs. In An_{70} Ardnamurchan plagioclase the $I\bar{1}$ phase has ordered further upon cooling to the periodic antiphase structure. Plagioclase with composition An_{75}–An_{78} from Ardnamurchan contains large micron-sized $I\bar{1}$ domains separated by APBs (Grove, 1977, Fig. 6). The An_{78} first ordered to $I\bar{1}$, then decomposed within the conditional spinodal and produced oriented lamellae. In regions of bytownite (An_{80-81}) large APBs are decorated with an Na-rich $C\bar{1}$ phase (Grove, 1977, Fig. 7). The bytownite lies outside the spinodal in a region of metastability, and the disordered phase nucleated heterogeneously on the APBs. Subsequently the $C\bar{1}$ phase ordered to the periodic antiphase structure. These observations place the tricritical point for $C\bar{1} \rightarrow I\bar{1}$ near An_{75}.

The temperature of the tricritical point must be between the temperatures at which the plutonic plagioclase crystallized (~1100°C) and the temperatures at which the metamorphic plagioclase crystallized (~650°C, discussed in a later section). Experimental evidence (Orville, 1972; Goldsmith, 1982) places the point above 700°C. The results of annealing experiments performed on a volcanic labradorite (Wenk, 1978) set further limits on the temperature of the tricritical point. Wenk found that hydrothermal annealling at 850°C and 2000 bars for 50 days caused the labradorite to unmix into $I\bar{1}$ and intermediate plagioclase. A temperature of ~900°C for the $C\bar{1} \rightleftarrows I\bar{1}$ tricritical point is consistent with all the above constraints. Figures 8 and 9a show our estimated position of the tricritical point on a proposed T–X diagram for the calcic portion of the system $NaAlSi_3O_8$–$CaAl_2Si_2O_8$. By analogy with Figure 7, Figures 8 and 9a contain appropriate curves which must radiate from the tricritical point.

The tricritical point associated with the $I\bar{1} \rightleftarrows P\bar{1}$ transition. A tricritical point associated with the $I\bar{1} \rightleftarrows P\bar{1}$ transition in plagioclase must occur at a temperature below that of the $C\bar{1} \rightleftarrows I\bar{1}$ tricritical point because the $I\bar{1} \rightleftarrows P\bar{1}$ transition curve always lies at a lower temperature than the $C\bar{1} \rightleftarrows I\bar{1}$ transition curve for a given composition. Because Huttenlocher intergrowths involve coexisting $P\bar{1}$ and $I\bar{1}$ feldspars, we associate Huttenlocher intergrowths with phase decomposition at temperatures below the $P\bar{1} \rightleftarrows I\bar{1}$ tricritical point. Data on the Huttenlocher intergrowths therefore permit approximate location of the $P\bar{1} \rightleftarrows I\bar{1}$ tricritical point in T–X space. Huttenlocher intergrowths are composed of plagioclase of composition ~An_{66} coexisting with plagioclase of composition ~An_{87}. We therefore locate the $I\bar{1} \rightleftarrows P\bar{1}$ tricritical point midway between these compositions at ~An_{77}. Huttenlocher intergrowths are observed in metamorphic plagioclase crystallized at $T \sim 650$°C (Grove, 1977). We therefore locate the $I\bar{1} \rightleftarrows P\bar{1}$ tricritical point above this temperature but below 900°C, the temperature of the $C\bar{1} \rightleftarrows I\bar{1}$ tricritical point. Figures 8 and 9a show our estimated position of the tricritical point on proposed T–X diagrams for the calcic portion of the system $NaAlSi_3O_8$–$CaAl_2Si_2O_8$. By analogy with Figure 7, appropriate curves are shown radiating from the tricritical point.

Figures 8 and 9a illustrate two possible interpretations of the $I\bar{1} \rightleftarrows P\bar{1}$ tricritical point which are both consistent with existing data for plagioclase feldspars. In Figure 8, in analogy to phase relations in the system Fe–Al, the $I\bar{1} \rightleftarrows P\bar{1}$ tricritical point is shown as metastable. The experiments of Goldsmith (1982) show no evidence for stable Bøggild or Huttenlocher gaps at P = 7000–9000 bars; T = 700–1000°C but are consistent with a wide $C\bar{1}$–$P\bar{1}$ two-phase region at temperatures as low as 700°C. Goldsmith's experiments therefore support Figure 8 in which the $I\bar{1} \rightleftarrows P\bar{1}$ tricritical point is metastable. Data of Wenk and Wenk (1977), on the other hand, suggest a stable Bøggild miscibility gap and therefore support Figure 9a in which the $I\bar{1} \rightleftarrows P\bar{1}$ tricritical point is stable. Compositional data on coexisting calcic plagioclase feldspars (Fig. 1) are consistent with the topology of either Figure 8 or Figure 9a. As mentioned earlier, a stable $I\bar{1} \rightleftarrows P\bar{1}$ tricritical point could be confidently endorsed if the existence of stable coexisting An_{45} + An_{65} feldspar could ever be demonstrated.

Model phase diagrams. Figures 8 and 9 summarize our best estimates of subsolidus phase relations in the calcic portion of the albite–anorthite system. Existing data are consistent with either of these phase diagrams. It may turn out that one or the other is correct for P–T conditions that are present in planetary crusts. Alternatively, Figure 8 may correctly illustrate phase relations at high pressures while Figure 9a correctly illustrates phase relations at low pressures. If the latter interpretation is correct, then the $I\bar{1} \rightleftarrows P\bar{1}$ tricritical point, the $C\bar{1} \rightleftarrows I\bar{1}$ tricritical point, and the univariant three-phase equilibrium among $C\bar{1}$, $I\bar{1}$, and $P\bar{1}$ plagioclase must trace out curves in P–T space as shown in Figure 9b. T–X diagrams with a topology like Figure 8 would be correct at pressures such as P_2 in Figure 9b; T–X diagrams with a topology like Figure 9a would be correct at lower pressures such as P_1.

Microstructures in calcic plagioclase: TEM observations and interpretation using model phase diagrams

In this section voluminous data on microstructures in calcic plagioclase are reviewed. A variety of TEM observations can be explained readily by stable and metastable ordering and decomposition sequences predicted by Figures 8 and 9a.

Calcic plagioclase in igneous rocks

The slow cooling rates experienced by plagioclases from large igneous intrusives produce distinctive TEM microstructures. Grove (1977) found sparsely distributed lamellae of calcic $I\bar{1}$ plagioclase in An_{66-70} Nain plagioclase (Fig. 10a). This compo-

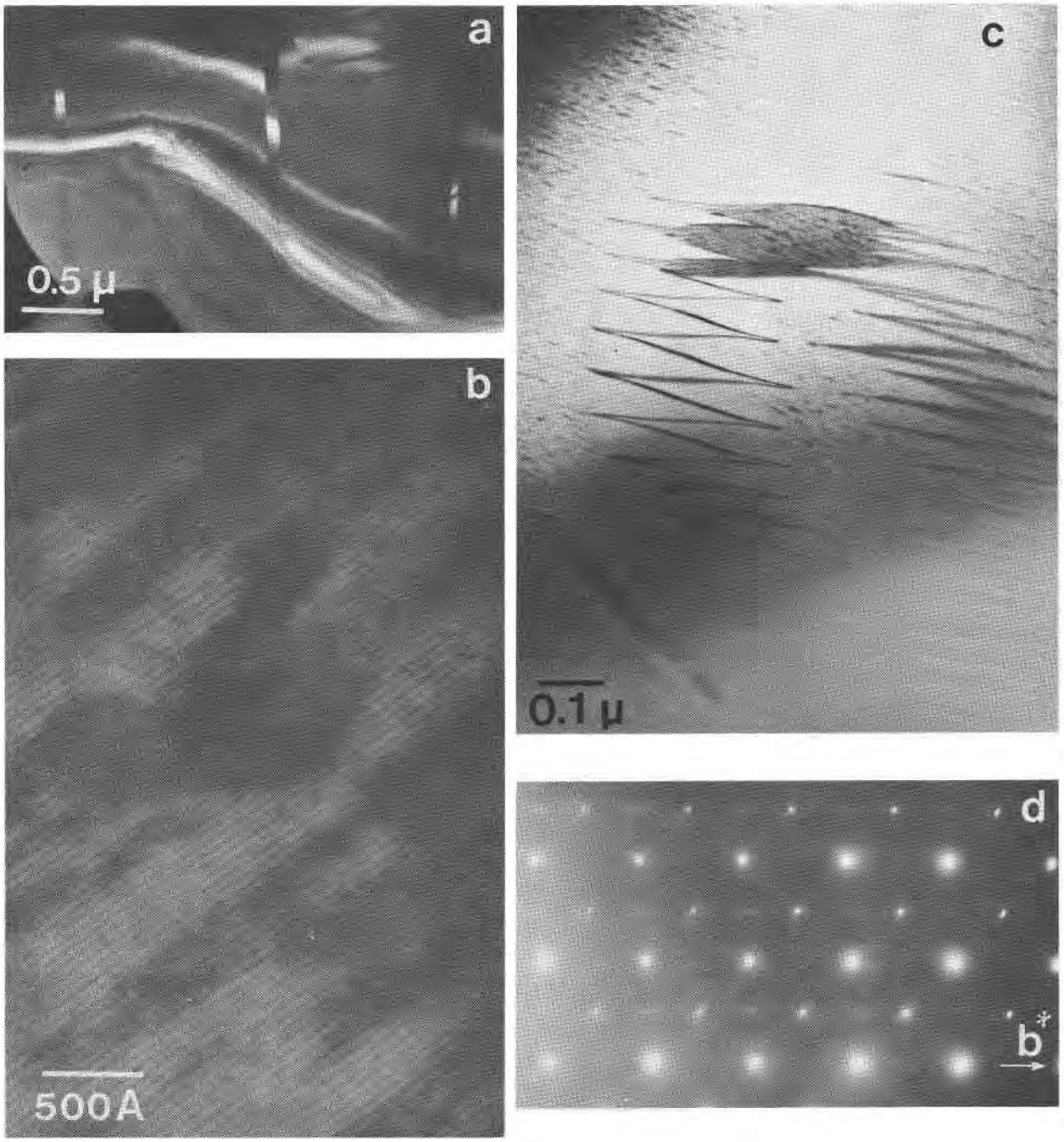

Fig. 10. TEM observations of plutonic plagioclase. (a) Nain plagioclase An_{66-70} contains isolated lamellae of the calcic phase. DF, $g = 0\bar{1}3$. (b) Nain labradorite An_{72}. Two phase intergrowth of $C\bar{1}$ and $I\bar{1}$ formed by cooling into the conditional spinodal from the stability field of $C\bar{1}$. Ordering on $I\bar{1}$ produces APBs, which on decomposition are wetted by the $C\bar{1}$ phase. Because the $I\bar{1}$ periodic antiphase domains overlap, it is not possible to see the regions of $C\bar{1}$. Light regions are inferred to be $I\bar{1}$, dark regions are inferred to be $C\bar{1}$. DF, $g = 02\bar{2}$. (c) Stillwater bytownite An_{82}. Zigzag b APBs have served as sites for heterogeneous nucleation of $C\bar{1}$ phase. The $C\bar{1}$ phase has transformed to the periodic antiphase structure as seen by the periodicity on the APB (upper center). Within $I\bar{1}$ ordered domains metastable $P\bar{1}$ and $I\bar{1}$ decomposition has occurred. Regions adjacent to the APB are devoid of these precipitates. DF, $g = 031$. (d) [100] selected area diffraction pattern of Stillwater bytownite. The diffuse c reflections indicate $P\bar{1}$ symmetry. b^* is horizontal and c^* is vertical.

sition lies in the metastable portion of the $C\bar{1} \rightarrow I\bar{1}$ conditional spinodal. The ordered calcic phase formed by heterogeneous nucleation, which occurred randomly on defects in the disordered phase and produced the observed texture. In slightly more calcic bulk compositions An_{72-75} (Fig. 10b) the microstructure was produced by ordering below the metastable extension of the $C\bar{1} \rightarrow I\bar{1}$ transition. The small APD size was on the order of the spinodal wavelength, and the disordered phase wetted the APBs, producing a connected intergrowth of $C\bar{1}$ with isolated $I\bar{1}$ cores. Subsequent ordering of $I\bar{1}$ domain cores on the periodic antiphase structure produced the observed superlattice periodicity.

Some slowly cooled plutonic plagioclase undergo $C\bar{1} \rightarrow I\bar{1}$, grow with large $I\bar{1}$ ordered domains and then enter the $C\bar{1}$–$I\bar{1}$ two phase region as cooling continues. The compositions of these plagioclases (An_{78} to An_{80}) lie outside the $C\bar{1}$–$I\bar{1}$ conditional spinodal, but inside the two phase region, so that heterogeneous nucleation of the $C\bar{1}$ phase on the $I\bar{1}$ APB can occur. Textures consistent with this transition sequence are found in bytownite from Nain (Grove, 1977, Fig. 9) and the Stillwater igneous complex (Nord *et al.*, 1974). The $I\bar{1}$ APBs are wetted by $C\bar{1}$ (Fig. 10c) which later transformed on the $I\bar{1}$ periodic APB structure. Further decomposition occurs on cooling and a spinodal texture forms within the $I\bar{1}$ domains, which consists of intergrown $P\bar{1}$ and $I\bar{1}$ with the periodic antiphase structure (Fig. 10d). The transition sequence described above for bytownite (An_{80-85}) would be predicted by Fig. 8. Ordering from $C\bar{1}$ to $I\bar{1}$ occurs and APDs form. Subsequent cooling places the $I\bar{1}$ domains within the conditional spinodal for $P\bar{1}$ and $I\bar{1}$, and decomposition occurs within the $I\bar{1}$ domains. Ordering within the conditional spinodal forms $P\bar{1}$ domains and decomposition of an $I\bar{1}$ Na-rich phase. The topology suggested in Fig. 8 interprets the $I\bar{1} + P\bar{1}$ two-phase intergrowth as metastable with respect to an equilibrium assemblage of $C\bar{1} + P1$, which could form by nucleation and growth. The lamellar orientation of the spinodal texture parallels that predicted for the minimization of interfacial strain energy (Williame and Brown, 1974). The $P\bar{1}$ domains are less than 100Å in width and are elongate parallel to (010). This $P\bar{1}$ APB orientation does not correspond to one in which the strain energy is minimized and is not an orientation for coarsening of lamellae.

Bøggild intergrowths (McConnell, 1974b) are found in labradorites (An_{50-55}) and contain coexisting An_{45} and An_{65} plagioclase. These intergrowths suggest that the $C\bar{1}$–$I\bar{1}$ conditional spinodal extends into the sodium-rich portion of the diagram (Fig. 8, 9a). The Bøggild intergrowths form by ordering within the conditional spinodal below the metastable extension of the $C\bar{1} \rightarrow I\bar{1}$ transition. Ordering of $C\bar{1}$ creates small $I\bar{1}$ domains and abundant APBs. Spinodal decomposition to $C\bar{1} + I\bar{1}$ follows. In labradorites that contain small APDs the Na-rich disordered phase wets the $I\bar{1}$ domain boundaries forming an interconnected region of $C\bar{1}$ and isolated volumes of the $I\bar{1}$ phase. In labradorites with large $I\bar{1}$ APDs, decomposition results in oriented lamellar intergrowths. The calcic phase or both phases reequilibrate at low temperatures and order on the periodic antiphase structure. TEM observations of Bøggild intergrowths (Hashimoto *et al.* 1976, Fig. 1; Wenk and Nakajima, 1980, Fig. 2c) show the mottled texture characteristic of $I\bar{1}$ APB ordering followed by decomposition below the metastable extension of the $C\bar{1} \rightarrow I\bar{1}$ line in the conditional spinodal. Many intermediate plagioclases show evidence of this transition sequence. For example, the textures observed by Grove (1976, Fig. 1c,d) in metamorphic An_{66}, the TEM microstructures observed by McLaren and Marshall (1974, Fig. 7) in An_{32}, the textures in Thetford An_{39} (Fig. 4d) and the Augusta An_{50} (Fig. 6b) can be produced by ordering to $I\bar{1}$ within the Bøggild conditional spinodal followed by unmixing of a $C\bar{1}$ phase that wets the preexisting $I\bar{1}$ APBs.

Calcic plagioclase in metamorphic rocks

The Thetford two-plagioclase intergrowths are evidence that the An_{39}–An_{88} assemblage is stable and that the Huttenlocher intergrowths formed metastably. As discussed in the previous section microstructures observed in the An_{39} phase may be metastably precipitated $C\bar{1} + I\bar{1}$. The *G–X* diagrams (Fig. 11) show many possibilities for metastable behavior, and suggest a transition sequence that produced the TEM microstructures observed in Thetford plagioclase. Equilibrium $C\bar{1}$ (An_{39}) and $P\bar{1}$ (An_{88}) plagioclase nucleated and grew during prograde reaction. Continued plagioclase growth surrounded the An_{39} grains, removing them from reaction and the calcic plagioclase grew into the Na-rich region of instability. Spinodal decomposition occurred within the $I\bar{1}$–$P\bar{1}$ conditional spinodal and produced the metastable Huttenlocher inter-

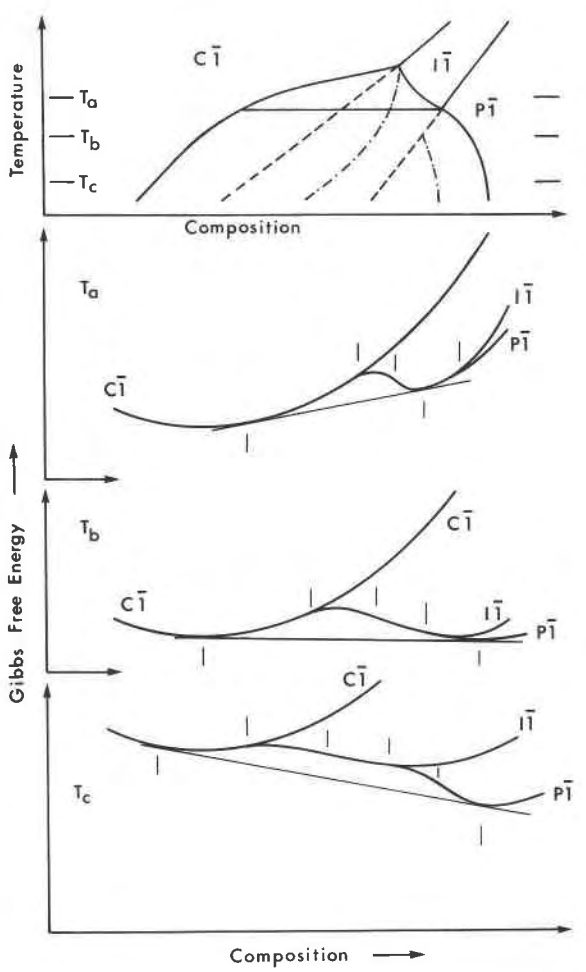

Fig. 11. Free energy (G)-composition diagrams show possibilities for metastability. For selected isotherms on the schematic T–X diagram G–X diagrams are constructed below. T_a shows G–X curves at a temperature below the $C\bar{1}$–$I\bar{1}$ tricritical point. T_b shows G–X curves above the $P\bar{1}$–$I\bar{1}$ tricritical point, but below the intersection of the $P\bar{1}$ stability field with the two-phase region. T_c shows G–X curves at a temperature below both tricritical points. Tangent planes show the equilibrium compositions of two-phase assemblages that define the miscibility gap. Vertical marks below the tangent surface emphasize the compositions. Vertical marks above the G-curves show the stable and metastable transition points and spinodals.

growths. Finally, decomposition of the An_{39} occurred on cooling below the metastable extension of the $C\bar{1} \rightleftarrows I\bar{1}$ ordering transition and produced metastable Bøggild precipitation.

Discussion and conclusions

Through consideration of the G–X curves in Figure 11 it is evident that metastable phenomena should be common in the plagioclase system. The T_a isotherm is constructed to pass through the $C\bar{1} \rightleftarrows I\bar{1}$ conditional spinodal. After ordering to $I\bar{1}$, compositions lying within the spinodal decompose to disordered $C\bar{1}$ and ordered $I\bar{1}$ plagioclases. The T_b isotherm intersects the two-phase field below the $I\bar{1} \rightleftarrows P\bar{1}$ transition. The conditional spinodal moves to progressively more sodic bulk compositions with decreasing temperature, and a large region exists over which the $I\bar{1}$ phase is metastable with respect to $P\bar{1} + C\bar{1}$. A bulk composition on the Ca-rich side of the spinodal can transform to $P\bar{1} + C\bar{1}$ only by heterogeneous nucleation. At T_c the metastable conditional spinodal for $I\bar{1}$–$P\bar{1}$ is intersected. Bøggild intergrowths are produced by ordering on $I\bar{1}$ followed by decomposition to a metastable assemblage of $C\bar{1}$ and $I\bar{1}$, where the $C\bar{1}$ phase has wetted the $I\bar{1}$ domain boundaries. The textures of these labradorite intergrowths (see Hashimoto, 1976, Fig. 1, Wenk and Nakajima, 1980, Fig. 4) and Augusta labradorite (Fig. 6b) are strikingly similar to those produced by the same transition mechanism in more calcic bulk compositions (Fig. 10b). The inability of some investigators to find 2e plagioclases in Bøggild intergrowths (Hashimoto *et al.*, 1976 vs McConnell, 1974b) is consistent with the formation of a periodic antiphase structure in the calcic $I\bar{1}$ phase and wetting of APBs by the disordered $C\bar{1}$ phase. The $C\bar{1}$ phase is the member of the Bøggild gap that lacks the e reflections.

As proposed in the preceding section the topology for the phase diagram in Figure 8 also shows Huttenlocher intergrowths as a metastable assemblage of coexisting $P\bar{1}$ and $I\bar{1}$ periodic antiphase plagioclase which should unmix to $C\bar{1} + P\bar{1}$. The persistence of Huttenlocher intergrowths is a consequence of the extremely slow interdiffusion of the NaSi and CaAl couple, and the existence of large activation energy barriers for heterogeneous nucleation. The metastable assemblage forms by spinodal decomposition, and further equilibration can occur only by nucleation and growth, as in the case of the Thetford plagioclase assemblage.

Our proposed phase diagrams are consistent with the 700°C, 2 kbar chloride exchange equilibria of Orville (1974). He found that plagioclase coexisting with aqueous chloride solutions could be modeled as disordered albite over the range An_0 to An_{55} and as ordered plagioclase over the range An_{85} to An_{100}. Intermediate compositions implied an equilibrium of two phases. Similarly, Goldsmith (1982) found evidence for an even wider gap at 700°C and P = 7 to 9 kbar in his experiments on the plagioclase–zoisite–kyanite–quartz–H_2O equilibrium. Our

results and the temperature–composition information for peristerites (Carpenter, 1981) may be combined to infer low temperature equilibria. At temperatures below 400°C, there exists a univariant equilibrium among $P\bar{1}$ anorthite, $C\bar{1}$ disordered andesine and $C\bar{1}$ ordered albite. Below this univariant line $C\bar{1}$ ordered albite and $P\bar{1}$ anorthite are the equilibrium phases. This assemblage may be difficult to find in metamorphic rocks and would be produced by reaction mechanisms which involved nucleation.

An important consequence of the existence of the two-plagioclase region under metamorphic conditions is that in many assemblages there is an added constraint on the chemical potential of the plagioclase components. Ferry (1979) exploited this constraint in his analysis of solid-fluid equilibria in the Blue Rock Quarry, and Spear (1980,1981,1982) has explored the consequences in the graphical analysis of amphibolite assemblages. Consideration of such an equilibrium constraint on plagioclase assemblages may assist in determining the temperature, pressure and fluid composition during metamorphism.

To conclude, plagioclase microstructures observed by TEM have presented mineralogists with a confusing variety of textural relations. Using the proposed phase diagram, our interpretation implies that much of the submicroscopic observational data merely outlines the limits for metastable behavior, and shows the existence of two metastable conditional spinodals. Submicroscopic textures delineate the positions of conditional spinodals and record metastable equilibria. We note that the topology of any phase diagram may vary according to T, P, and η (the degree of ordering in the plagioclase) and the phase diagrams suggested here are only one set among a range of possible topologies. Carpenter (1981) shows a range of possibilities for the peristerite spinodal, and a similar line of reasoning applies to conditional spinodals in the calcic portion of the system. Metamorphic plagioclase assemblages, on the other hand, may contain information on the equilibrium phase coexistences, when evidence for heterogeneous nucleation and exchange equilibrium with coexisting silicates can be shown. This evidence requires careful petrographic and analytical work as these plagioclase assemblages are often difficult to identify and may be complicated by continued reaction that departs from equilibrium. The results of this study serve to re-emphasize several aspects of equilibria in the plagioclase system. Plagioclase is extremely susceptible to decomposition to metastable intergrowths which may then persist for long periods ($>10^9$ years). The submicroscopic textural information recorded by plagioclase, while useful in recording the time–temperature path followed during the sample's formation history, may often be a record of metastable rather than stable equilibrium. Traditionally, mineralogists have thought that equilibration reactions within the plagioclase system involve ordering. It is ironic that under equilibrium conditions of low temperature regional metamorphism a region of stability for disordered andesine and $P\bar{1}$ bytownite exists. At lower temperatures, however, the proposed ordered albite + $P\bar{1}$ anorthite assemblage presumably exists.

References

Allen, J. M. and Fawcett, J. J. (1982) Zoisite–anorthite–calcite stability relations in H_2O–CO_2 fluids at 5000 bars: an experimental and SEM study. Geochimica et Cosmochimica Acta, in press.

Allen, S. M. (1977) Phase separation of Fe–Al alloys with Fe_3Al order. Philosophical Magazine, 36, 181–192.

Allen, S. M. and Cahn, J. W. (1976a) Mechanisms of phase transformations within the miscibility gap of Fe-rich Fe–Al alloys. Acta Metallurgica, 24, 425–437.

Allen, S. M. and Cahn, J. W. (1976b) On tricritical points resulting from the intersection of lines of higher-order transitions with spinodals. Scripta Metallurgica, 10, 451–454.

Bown, M. G. and Gay, P. (1958) The reciprocal lattice geometry of the plagioclase feldspar structures. Zeitschrift für Kristallographie, 111, 1–14.

Bruno, E., Chiari, G. and Facchinelli, A. (1976) Anorthite quenched from 1530°C I. Structure refinement. Acta Crystallographica, B32, 3270–3280.

Carpenter, M. A. (1981) A "conditional spinodal" within the peristerite miscibility gap of plagioclase feldspars. American Mineralogist, 66, 553–560.

Cliff, G., Champness, P. E., Nissen, H. U. and Lorimer, G. W. (1976) Analytical electron microscopy of exsolution lamellae in plagioclase feldspar. In H.-R. Wenk, Ed., Electron Microscopy in Mineralogy, p. 258–265. Springer-Verlag, New York.

Crawford, M. L. (1966) Composition of plagioclase and associated minerals in some schists from Vermont, USA and South Westland, New Zealand, with inferences about the peristerite solvus. Contributions to Mineralogy and Petrology, 13, 269–294.

Czank, M. (1973) Strukturen des Anorthits bei höhern Temperaturen. Thesis, E. T. H. Zürich.

Evans, B. W. (1964) Coexisting albite and oligoclase in some schists from New Zealand. American Mineralogist, 49, 173–179.

Ferry, J. M. (1976) P, T, f_{CO_2} and f_{H_2O} during metamorphism of calcareous sediments in the Waterville–Vassalboro area, South Central Maine. Contributions to Mineralogy and Petrology, 57, 119–143.

Ferry, J. M. (1979) A map of chemical potential differences within an outcrop. American Mineralogist, 64, 966–985.

Ferry, J. M. (1980a) A case study of the amount and distribution of heat and fluid during metamorphism. Contributions to Mineralogy and Petrology, 71, 373–385.

Ferry, J. M. (1980b) A comparative study of geothermometers and geobarometers in pelitic schists from South-central Maine. American Mineralogist, 65, 720–732.

Fleet, M. E. (1981) The intermediate plagioclase structure: an explanation from interface theory. Physics and Chemistry of Minerals, 7, 64–70.

Foit, F. F. and Peacor D. R. (1967) High temperature diffraction data on selected reflections of an andesine. Zeitschrift für Kristallographie, 125, 1–6.

Foit, F. F. and Peacor, D. R. (1973) The anorthite crystal structure at 410° and 830°C. American Mineralogist, 58, 665–675.

Gay, P. (1953) The structures of the plagioclase feldspars. III. An x-ray study of anorthites and bytownites. Mineralogical Magazine, 30, 169–177.

Goldsmith, J. R. (1982) Plagioclase stability at elevated temperatures and water pressures. American Mineralogist, 67, 652–675.

Grove, T. L. (1976) Exsolution in metamorphic bytownite. In H.-R. Wenk, Ed., Electron Microscopy in Mineralogy, p. 266–270. Springer-Verlag, New York.

Grove, T. L. (1977) Structural characterization of labradorite–bytownite plagioclase from volcanic, plutonic and metamorphic environments. Contributions to Mineralogy and Petrology, 64, 273–302.

Hashimoto, H., Nissen, H.-U., Ono, A., Kumao, A., Endoh, H. and Woensdregt, C. F. (1976) High-resolution electron microscopy of labradorite feldspar. In H.-R. Wenk, Ed., Electron Microscopy in Mineralogy, p. 332–344. Springer-Verlag, New York.

Heuer, A. H. and Nord, G. L., Jr. (1976) Polymorphic phase transitions in minerals. In H.-R. Wenk, Ed., Electron Microscopy in Mineralogy, p. 274–303. Springer-Verlag, New York.

Heuer, A. H., Nord, G. L. Jr., Lally, J. S. and Christie, J. M. (1976) Origin of the (c) domains of Anorthite. In H.-R. Wenk, Ed., Electron Microscopy in Mineralogy, p. 345–353. Springer-Verlag, New York.

Korekawa, M., Horst, W. and Tagai, T. (1978) Superstructure of labradorite $An_{\sim 50}$. Physics and Chemistry of Minerals, 3, 74–75.

Lally, J. S., Fisher, R. M., Christie, J. M., Griggs, D. T., Heuer, A. H., Nord, G. L., Jr. and Radcliffe, S. V. (1972) Electron petrography of Apollo 14 and 15 rocks. Proceedings of the 3rd Lunar Science Conference, 401–422.

Landau, L. D. and Lifshitz, E. M. (1958) Statistical physics. Addison Wesley, Reading Massachusetts.

Laves, F. and Goldsmith, J. R. (1951) Short range order in anorthite. (abstr.) American Crystallographic Association Meeting, Chicago, 10.

McConnell, J. D. C. (1974a) Analysis of the time-temperature-transformation behavior of the plagioclase feldspars. In W. S. MacKenzie and J. Zussman, Eds., The Feldspars, p. 460–477. Manchester University Press, Manchester.

McConnell, J. D. C. (1974b) Electron optical study of the fine structure of a Schiller labradorite. In W. S. MacKenzie and J. Zussman, Eds., The Feldspars, p. 478–490. Manchester University Press, Manchester.

McConnell, J. D. C. (1978) The intermediate plagioclase feldspars: an example of a structural resonance. Zeitschrift für Kristallographie, 147, 45–62.

McLaren, A. C. (1974) Transmission electron microscopy of the Feldspars. In W. S. MacKenzie and J. Zussman, Eds., The Feldspars, p. 378–423. Manchester University Press, Manchester.

McLaren, A. C. and Marshall, D. B. (1974) Transmission electron microscope study of the domain structure associated with the *b*-, *c*-, *d*-, *e*- and *f*- reflections in plagioclase feldspar. Contributions to Mineralogy and Petrology, 44, 237–249.

Müller, W. F. and Wenk, H.-R. (1973) Changes in the domain structure of anorthites induced by heating. Neues Jahrbuch für Mineralogie, Monatshefte, 17–26.

Nissen, H.-U. (1968) A study of bytownites in amphibolites of the Ivrea-zone (Italian alps) and in anorthosites: A new unmixing gap in the low plagioclases. Schweizerische Mineralogische und Petrographische Mitteilungen, 48, 53–56.

Nissen, H.-U. (1974) Exsolution phenomena in bytownite plagioclase. In W. S. MacKenzie and J. Zussman, Eds., The Feldspars, p. 491–521. Manchester University Press, Manchester.

Nord, G. L. Jr., Heuer, A. H. and Lally, J. S. (1974) Transmission electron microscopy of substructures in Stillwater bytownites. In W. S. MacKenzie and J. Zussman, Eds., The Feldspars, p. 522–535. Manchester University Press, Manchester.

Nord, G. L. Jr., Lally, J. S., Heuer, A. H., Christie, J. M., Radcliffe, S. V., Griggs, D. T. and Fisher, R. M. (1973) Petrologic study of igneous and metaigneous rocks from Apollo 15 and 16 using high voltage transmission electron microscopy. Proceedings of the Fourth Lunar Science Conference, 953–970.

Orville, P. M. (1972) Plagioclase cation exchange equilibria with aqueous chloride solution: results at 700°C and 2000 bars in the presence of quartz. American Journal of Science, 272, 234–272.

Ribbe, P. H. (1975) The chemistry, structure and nomenclature of feldspars. In P. H. Ribbe, Ed., Reviews in Mineralogy, V. 2, Feldspars, p. R1–R72. Mineralogical Society of America, Washington D.C.

Rumble, D., Ferry, J. M., Hoering, T. C. and Boucot, A. J. (1982) Fluid flow during metamorphism at the Beaver Brook fossil locality, New Hampshire. American Journal of Science, 282, 886–919.

Slimming, E. H. (1976) An electron diffraction study of some intermediate plagioclases. American Mineralogist, 61, 54–59.

Smith, J. V. (1972) Critical review of synthesis and occurrence of plagioclase feldspars and a possible phase diagram. Journal of Geology, 80, 505–525.

Smith, J. V. (1974) Feldspar minerals. I. Crystal structure and physical properties. Springer-Verlag, Heidelberg.

Spear, F. S. (1980) $NaSi \rightleftharpoons CaAl$ exchange equilibrium between plagioclase and amphibole: an empirical model. Contributions to Mineralogy and Petrology, 72, 33–41.

Spear, F. S. (1981) Amphibole-plagioclase equilibria: an empirical model for the relation albite + tremolite = edenite + 4 quartz. Contributions to Mineralogy and Petrology, 77, 355–364.

Spear, F. S. (1982) Phase equilibria of amphibolites from the Post Pond Volcanics, Mt. Cube Quadrangle, Vt., Journal of Petrology, 23, 383–426.

Walker, D., Longhi, J., Grove, T. L., Stolper, E. and Hays, J. F. (1973) Experimental petrology and origin of rocks from Descartes Highlands. Proceedings of the Fourth Lunar Science Conference, 1013–1032.

Wenk, E. and Wenk, H.-R. (1977) An-variation and intergrowths of plagioclases in banded metamorphic rocks from Val Carec-

chio (central Alps). Schweizerische Minerlogische und Petrographische Mitteilungen, 57, 41–57.

Wenk, H.-R. (1978) Ordering of the intermediate plagioclase structure during heating. American Mineralogist, 63, 132–135.

Wenk, H.-R. (1979) Superstructure variation in metamorphic intermediate plagioclase. American Mineralogist, 64, 71–76.

Wenk, H.-R. and Nakajima, Y. (1980) Structure, formation and decomposition of APBs in calcic plagioclase. Physics and Chemistry of Minerals, 6, 169–186.

Wenk, H.-R., Joswig, W., Tagai, T., Korekawa, M. and Smith, B. K. (1980) The average structure of An_{62-66} labradorite. American Mineralogist, 65, 81–95.

Williame, C. and Brown, W. L. (1974) A coherent elastic model for the determination of the orientation of exsolution boundaries: application to the feldspars. Acta Crystallographica, A30, 316–331.

Manuscript received, February 24, 1982;
accepted for publication, September 6, 1982.